
**Liquid Crystals**
Publication details, including instructions for authors and subscription information:
http://www.informaworld.com/smpp/title~content=t713926090

# The effect of high electric fields on the structure and dielectric properties of the $B_2$ phase

S. Diez[a]; M. R. De La Fuente Corresponding author[a]; M. A. Pérez Jubindo[a]; B. Ros[b]
[a] Departamento de Física Aplicada II, Facultad de Ciencias, Universidad del País Vasco, 48 080 Bilbao, Spain [b] Departamento de Química Orgánica, Facultad de Ciencias-ICMA, Universidad de Zaragoza-CSIC, 50 009 Zaragoza, Spain

Online publication date: 07 July 2010

**To cite this Article** Diez, S. , De La Fuente Corresponding author, M. R. , Jubindo, M. A. Pérez and Ros, B.(2003) 'The effect of high electric fields on the structure and dielectric properties of the $B_2$ phase', Liquid Crystals, 30: 12, 1407 — 1412
**To link to this Article: DOI:** 10.1080/02678290310001622498
**URL:** http://dx.doi.org/10.1080/02678290310001622498

LIQUID CRYSTALS, VOL. 30, NO. 12, DECEMBER 2003, 1407–1412

Taylor & Francis
Taylor & Francis Group

# The effect of high electric fields on the structure and dielectric properties of the $B_2$ phase

S. DIEZ, M. R. DE LA FUENTE*, M. A. PÉREZ JUBINDO
Departamento de Física Aplicada II, Facultad de Ciencias, Universidad del País Vasco, Apdo. 644, 48 080 Bilbao, Spain

and B. ROS
Departamento de Química Orgánica, Facultad de Ciencias-ICMA, Universidad de Zaragoza-CSIC, 50 009 Zaragoza, Spain

(*Received 13 March 2003; in final form 4 June 2003; accepted 18 July 2003*)

Dielectric studies are presented of a banana-shaped compound that exhibits the antiferroelectric $B_2$ phase. Upon application and subsequent removal of strong electric fields the textures and dielectric properties of the phase drastically change. Most notable is the huge increase of the low frequency permittivity. This behaviour would suggest the induction of ferroelectricity by the electric field.



## 1. Introduction

Bent core molecules give rise to liquid crystalline compounds exhibiting unusual mesophases in which achiral molecules can form chiral and polar phases showing ferro- and antiferro-electricity [1–4]. Among them, the $B_2$ phase is one of the most studied: the molecules stack in layers and are tilted with respect to the layer normal. This shows antiferroelectric behaviour with the dipoles pointing in opposite directions in successive layers. In this paper we study an asymmetric bent-shaped compound (see structure below), whose synthesis has already been published [5]. Our DSC, X-ray and polarizing microscopy studies confirm the phase sequence reported previously: I (158°C) $B_2$ (70°C) X.

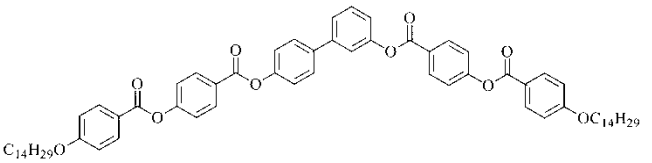


On entering the $B_2$ phase from the isotropic phase, a typical texture with small coloured domains and some fans is obtained, see figure 1 (*a*). On applying a field (similar to that needed to measure the spontaneous polarization, triangular, square or continuous) and then removing it, the new texture appears dark grey between

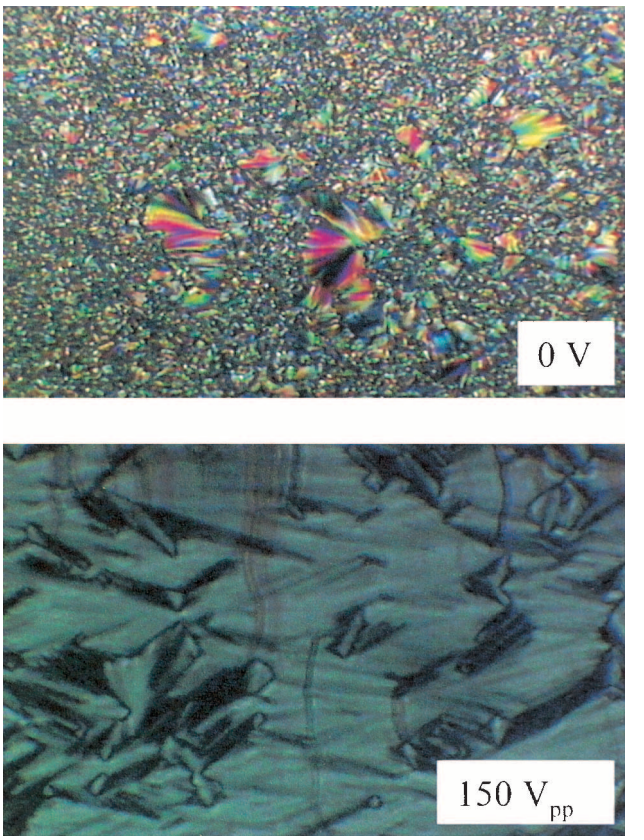


Figure 1. (*a*) Texture observed in the $B_2$ phase after cooling from the isotropic phase in the absence of an electric field. (*b*) Effect on the texture of a triangular voltage (50 Hz).

*Author for correspondence; e-mail: wdpfular@lg.ehu.es

*Liquid Crystals* ISSN 0267-8292 print/ISSN 1366-5855 online © 2003 Taylor & Francis Ltd
http://www.tandf.co.uk/journals
DOI: 10.1080/0267829031000162249 8

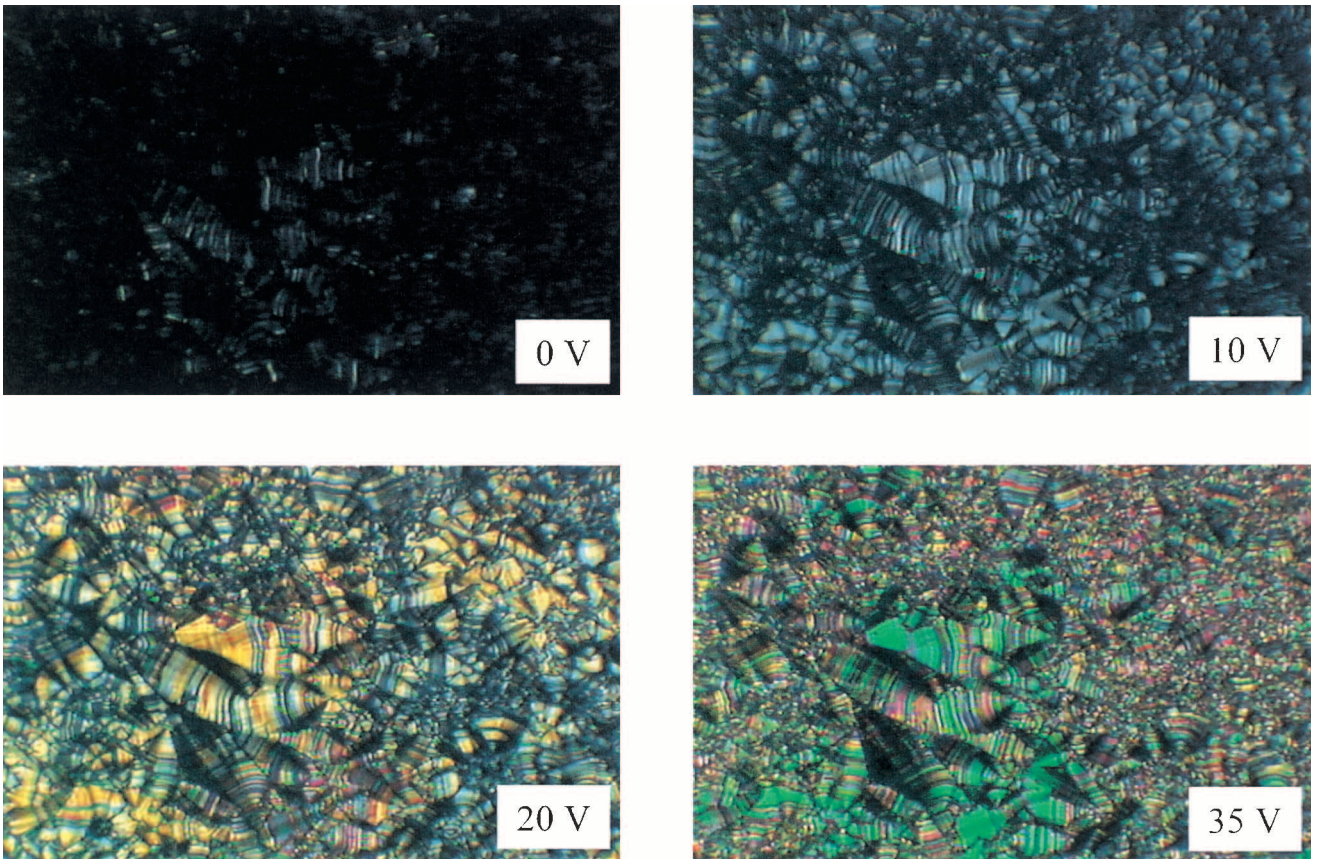


Figure 2. Textures observed in the $B_2$ phase upon field removal of a high d.c. voltage (100 V) and further application of different d.c. voltages.



crossed polarizers, see figure 2 (*a*). The aspect is darker if the field is applied from the isotropic phase. This extinction does not change when the sample is rotated. On uncrossing the polarizer and analyser by a few degrees, two types of domain, without birefringence but with opposite optical rotation, can be distinguished. Under the application of low amplitude triangular fields (much smaller than needed to switch the polarization) reversible changes can be observed in the texture. It can be seen that the birefringence increases and that the focal-conics containing fringe patterns are perfectly visible, see figure 2. Some Maltese crosses can also be observed. These crosses rotate continuously following the field but in opposite directions depending on the chirality of the different domains. When the fields are high enough to invert the polarization, the texture is similar to the fan-shaped texture of a SmA phase, see figure 1 (*b*). All these facts, together with the dielectric behaviour that we will present later, strongly suggest the induction of ferroelectricity [6] and the presence of helical arrangements. In [7] a detailed electro-optic study of this compound has already been presented.

## 2. Experimental results and discussion

We measured spontaneous polarization using the triangular wave method with EHC cells (5 μm); this is almost constant over the whole range of the $B_2$ phase, with a value of around 900 nC cm$^{-2}$. Figure 3 shows

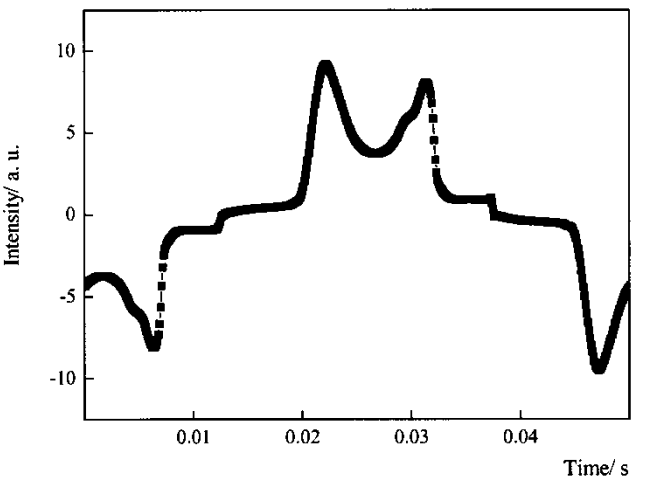


Figure 3. Polarization reversal current; triangular wave, 20 Hz, $V_{pp} = 240$ V.

a typical plot of the reversal polarization current (triangular wave, 20 Hz, 48 $V_{pp}\,\mu m^{-1}$); two main peaks, typical of antiferroelectric behaviour, are seen but with some fine structure. Specifically, one shoulder on each main peak can be observed. This fine structure depends greatly on frequency, maximum field applied and also on the previous field and thermal treatments. This behaviour was observed by other authors [8] and interpreted in terms of different kinds of domain in the material (racemic and homochiral). It is also interesting to note the high value of the current in between the two main peaks.

We measured the dielectric permittivity in the frequency range $10^2$–$10^7$ Hz using an HP4192A impedance analyser with two types of cell: cells with gold electrodes 50 μm thick, and ITO coated transparent cells 7 μm thick (commercially available EHC cells). The latter cells allow optical observation of the samples but are poorer electrically because of the ITO resistance ($R_{ITO}=10\,\Omega$ per square). We begin our observation with the metallic cells. Figure 4 is a three-dimensional plot of the imaginary part of the dielectric permittivity as a function of temperature and frequency. The measurements were taken under a bias field (0.7 $V\,\mu m^{-1}$) to quench the d.c. conductivity contribution. In the $B_2$ phase the spectrum is dominated by a relaxation around $10^6$ Hz near the isotropic phase but it shows strong thermal activation (mode h). Another relaxation mode at lower frequencies is also present (see figure 6). Mode h seems to come from one present in the isotropic phase at a higher frequency (it jumps one decade) and with smaller strength (around 1). This is presumably related to rotation around the long molecular axis. The stepwise decrease of the frequency at the I–$B_2$ phase transition may be understood in terms of the onset of the ordering of the short axes.

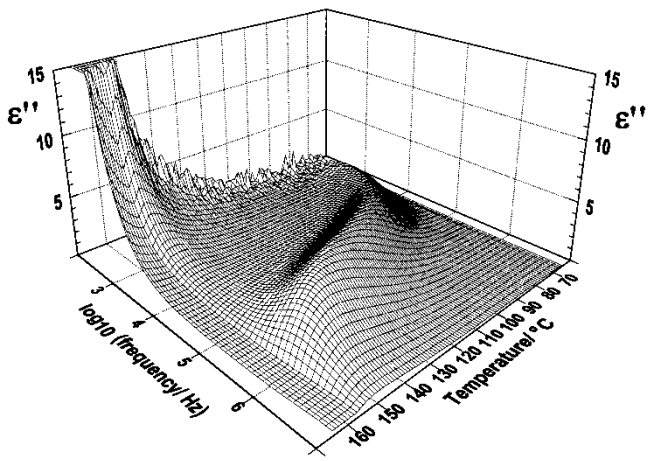


Figure 4. Dielectric loss as a function of temperature and frequency (gold electrodes) $V_{dc}=35$ V.

This behaviour was also observed at the I-SmA phase transition in brick-like compounds [9, 10] and was attributed to the biaxiality of the molecules. In that case, a potential with a quadrupolar term is seen by the molecules while rotating around their long axes and this is responsible for the ordering of the short axes. In a similar way, the order for the present compounds is imposed by steric hindrance, which may be considered to be the corresponding potential, and 'polar' due to the molecular bent shape [11]. Moreover, the dielectric strength of this mode is quite large when compared with the same mode in N, SmA or SmC* phases. We suggest that it is too large to be accounted for in terms of a 'pure molecular mode', but instead is related to collective motions of molecules with at least short range ferroelectric order. To determine the strengths and frequencies of the different modes, the experimental data of the complex dielectric permittivity were fitted to:

$$\varepsilon(\omega)=\sum_k \Delta\varepsilon_k(\omega)+\varepsilon_\infty-\mathrm{i}\sigma_{dc}/\omega\varepsilon_0 \qquad (1)$$

using simplex procedure. We fit simultaneously both components of the dielectric permittivity. $\Delta\varepsilon_k(\omega)$ accounts for the contribution of each mode, $\sigma_{dc}$ for the d.c. conductivity, and $\varepsilon_\infty$ for the high frequency permittivity. For $\Delta\varepsilon_k(\omega)$ we used the Cole–Cole function:

$$\Delta\varepsilon_k(\omega)=\frac{\Delta\varepsilon_k}{1+(\mathrm{i}\omega\tau)^\alpha} \qquad (2)$$

where $\Delta\varepsilon_k$ is the dielectric strength, $\tau$ the relaxation time and $\alpha$ controls the shape of the relaxation. In our case we fitted the data using two modes in addition to a d.c. conductivity contribution. The low frequency mode is a very broad one and not well defined for all temperatures.

In figure 5 we represent the frequency of the dominant mode h in an Arrhenius plot. It follows the Vogel–Fulcher–Tammann law: $f_k=f_{\infty k}\exp[-A/(T-T_0)]$ that in general is related to a glass transition [13]. $T_0$ is the so-called Vogel or ideal glass transition temperature (30–50 K below the calorimetric glass transition $T_g$) and $A$ is a constant. From the fit we obtained $T_0=299$ K, but this compound undergoes another phase transition before any vitrification occurred.

We have also performed dielectric studies with the EHC cells (7 μm) to observe the textures while making the measurements. The results obtained under a similar bias field are practically equal to those obtained in the metallic cells: the h mode plus a low frequency mode (a spurious contribution in the high frequency side due to the non-zero resistance of the ITO electrodes is also visible). In figure 5 we have also represented the

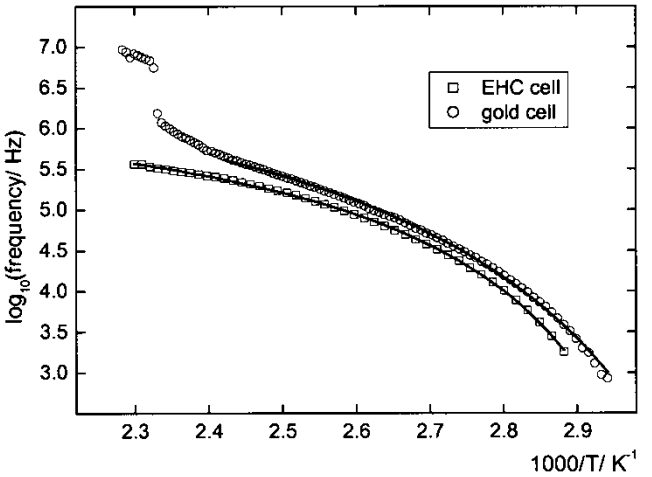


Figure 5. Arrhenius plot of the frequency of mode h: (○) gold electrodes, the solid line is the fit to the VFT law; (□) EHC cells with ITO electrodes.

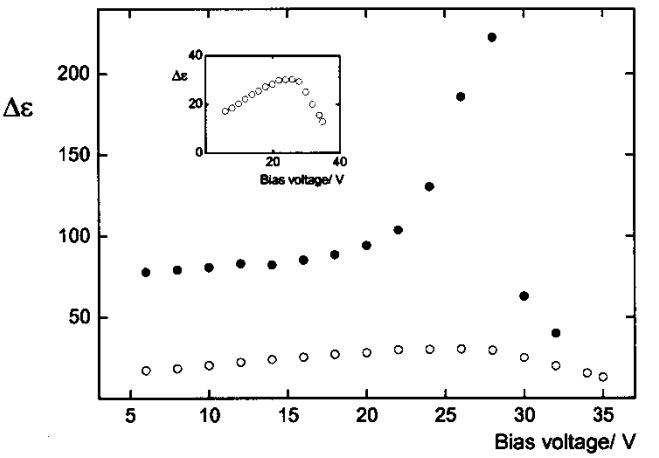


Figure 7. Dielectric strength of mode h vs. bias voltage (EHC cell): (○) no previous field treatment); (●) after field treatment.



frequency of mode h as obtained for these cells. It is smaller than for the metallic cells (this is an undesirable effect of the non-zero resistivity of the ITO electrodes and the shift is greater for large permittivities and high relaxation frequencies).

With these cells we have also measured the complex dielectric permittivity at selected temperatures in the $B_2$ phase under different bias voltages (0–35 V, the maximum allowed by our dielectric analyser) but just after cooling from the isotropic phase and before any previous field treatment. Figure 6 shows the complex dielectric permittivity as a function of frequency for 12 V at 135°C. The continuous lines are the fits to equations (1) and (2). Figure 7 shows the voltage dependence of the strength of mode h. We did not include in the plot the mode at the very low frequency side because, although it is always present, it is very broad and affected by the d.c. conductivity contribution. The strength of mode h first increases as the d.c. voltage increases, reaching a maximum value around 30 for 26 V but for larger fields decreases to values below that corresponding to zero field. Upon application and further removal of a high field (d.c., triangular or square) the behaviour changes dramatically (see figure 2).

Figure 8 shows the complex dielectric permittivity as a function of frequency for 12 V at 135°C (same conditions as figure 6 but after field treatment). Now

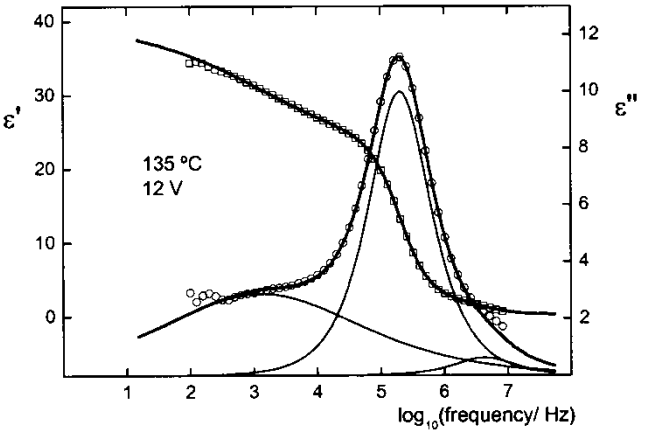


Figure 6. Complex dielectric permittivity at 135°C, $V_{dc} = 12$ V, EHC cell. The solid lines are fitted curves using equations (1) and (2).

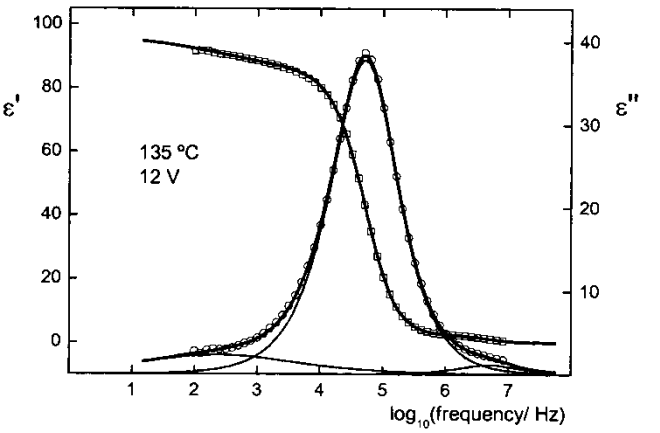


Figure 8. Complex dielectric permittivity at 135°C, after removal of a high d.c. voltage (100 V) and further application of 12 V, EHC cell. The solid lines are fit curves using equations (1) and (2).

the dielectric strength of the dominant mode is much larger than that seen in figure 6 (around 20 in figure 6 and around 80 in figure 8). The continuous lines are the fits to equations (1) and (2). The frequency of the dominant mode is smaller than before but we think that this is an 'artefact' due to the increasing capacitance of the cell. The field dependence of the strength follows a behaviour similar to that obtained prior to the high field treatment (see also figure 7): thus it initially increases as the d.c. voltage increases to 28 V, but for larger fields decreases to values below that corresponding to zero field. But now the strength reaches a value around 220 for 28 V then decreases quickly on increasing the d.c. voltage.

## 3. Summary

In summary, the dielectric response in the $B_2$ phase shows a relaxation that has been interpreted as due to rotation around the molecular long axes of the molecules. They have significant net transverse dipole moment and hence, one should expect a significant dielectric strength. In our case these strengths are around 15–20 at temperatures near the isotropic phase and we think that to explain these high values the molecules must have at least short range ferroelectric order, and the relaxation is somehow a co-operative process. Moreover, applying moderate d.c. fields (up to 35 V in 7 μm) these strengths first increase, but for larger fields decrease. To explain the increase of the dielectric strengths, solely an alignment effect of the field should be excluded.

More dramatic is the change induced by high fields. As discussed already, the application and subsequent removal of high electric fields induce irreversible changes in the textures and dielectric properties. The appearance of domains of different chirality, exhibiting girotropy and isotropy together with their electro-optic behaviour for low amplitude triangular waves is only possible if the phase is helical and ferroelectric [7]. Moreover the dielectric strengths increase from 20 prior to the field treatments to 80 after it. Now further application of moderate fields (up to 35 V in 7 μm cells) induces changes in the strengths: first an increase and for larger fields a decrease. The strength reaches a value around 220. We suggest that these high dielectric strengths are only possible if we are dealing with a type of 'collective helix-related ferroelectric mode'.

Although the field dependence is not exactly as expected for a Goldstone mode in an SmC* phase, we suggest that a helix-deformed ferroelectric mode is the only possible explanation. This prompts the question—how could this explanation be compatible with the data such as shown in figure 3? We believe that when measuring spontaneous polarization in these mesophases a very high field has always to be applied and then the samples always are in the 'field-induced state' (that corresponding to figure 2 and figure 8). The presence of two peaks instead of one in the reversal polarization current may be assigned to the helix recovery for low fields. This would also explain the high value of the current in between the two main peaks (zero-field region of the triangular wave) because it corresponds to a state with a very high value of the permittivity.

To conclude, we propose that a helical ferroelectric structure has been achieved through a field-induced 'learning of ferroelectricity' type effect [6]. This effect is much more pronounced when cooling from the isotropic phase with a high bias field applied. In this case antiferroelectricity does not seem to be present in the material, which behaves ferroelectrically. Chiral segregation is also induced as seen from the textures remaining upon field removal. In this state the dielectric spectrum is dominated by a mode with a very high dielectric strength whose field behaviour is similar to that of a conventional Goldstone mode in SmC* phases. The most probable state is a helical $SmC_SP_F$ phase (synclinic ferroelectric).

The Spanish Government, CICYT Project No. MAT 2000-1293-C02-(01 and 02), and the Universidad del País Vasco, Project No. 9/UPV00060.310-13562/2001, supported this work.

## References

[1] Niori, T., Sekine, T., Watanabe, J., Furukawa, T., and Takezoe, H., 1996, *J. mater. Chem.*, **6,** 1231.
[2] Link, D. R., Natale, G., Shao, R., Maclennan, J. E., Clark, N. A., Körblova, E., and Walba, D. M., 1997, *Science*, **278,** 1924.
[3] Pelz, G., Diele, S., and Weissflog, W., 1999, *Adv. Mater.*, **11,** 707.
[4] Dantlgraber, G., Eremin, A., Diele, S., Hauser, A., Kresse, H., Pelzl, G., and Tschierske, C., 2002, *Angew. Chem. int. Ed.*, **41,** 2408.
[5] Shen, D., Pegenau, A., Diele, S., Wirth, I., and Tschierske, C., 2000, *J. Am. chem. Soc.*, **122,** 1593.
[6] Gorecka, E., Pociecha, D., Glogarova, M., and Mieczkowski, J., 1998, *Phys. Rev. Lett.*, **81,** 2946.
[7] Etxebarria, J., Folcia, C. L., Ortega, J., and Ros, B., 2003, *Phys. Rev. E*, **67,** 04 2702.
[8] Barnik, M. I., Blinov, L. M., Shtykov, N. M., Palto, S. P., Pelzl, G., and Weissflog, W., 2002, *Liq. Cryst.*, **29,** 597.
[9] Pérez jubindo, M. A., de la Fuente, M. R., and Marcos, M., 1994, *Adv. Mater.*, **6,** 941.
[10] Merino, S., de Daran, F., de la Fuente, M. R., Pérez jubindo, M. A., Iglesias, R., and Marcos, M., 1996, *Adv. Mater.*, **8,** 644.

[11] KRESSE, H., SCHLACKEN, H., DUNEMANN, U., SCHRÖDER, M. W., PELZL, G., and WEISSFLOG, W., 2002, *Liq. Cryst.*, **29,** 1509.
[12] EREMIN, A., WIRTH, I., DIELE, S., PELZ, G., SCHMALFUSS, H., KRESSE, H., NÁDASI, H., FODOR-CSORBA, K., GÁCS-BAITZ, E., and WEISSFLOG, W, 2002, *Liq. Cryst.*, **29,** 775.
[13] GONZÁLEZ, Y., PALACIOS, B., PÉREZ JUBINDO, M. A., DE LA FUENTE, M. R., and SERRANO, J. L., 1995, *Phys. Rev. E*, **52,** R5764.